Acta Oceanol. Sin., 2019, Vol. 38, No. 4, P. 58–71
https://doi.org/10.1007/s13131-019-1413-7
http://www.hyxb.org.cn
E-mail: hyxbe@263.net

Seasonal and interannual variability of water mass sources of Indonesian throughflow in the Maluku Sea and the Halmahera Sea

Lu Wang[1, 2], Lei Zhou[3, 4], Lingling Xie[1]*, Quanan Zheng[5], Qiang Li[1], Mingming Li[1]

[1] Guangdong Key Laboratory of Coastal Ocean Variability and Disaster Prediction, Guangdong Ocean University, Zhanjiang 524088, China

[2] Department of Navigation, PLA Navy Petty Officer Academy, Bengbu 233012, China

[3] School of Oceanography, Shanghai Jiao Tong University, Shanghai 200240, China

[4] Laboratory for Regional Oceanography and Numerical Modeling, Pilot National Laboratory for Marine Science and Technology (Qingdao), Qingdao 266237, China

[5] Department of Atmospheric and Oceanic Science, University of Maryland, College Park, Maryland 20742, USA

Received 9 February 2018; accepted 27 April 2018

Abstract

So far, large uncertainties of the Indonesian throughflow (ITF) reside in the eastern Indonesian seas, such as the Maluku Sea and the Halmahera Sea. In this study, the water sources of the Maluku Sea and the Halmahera Sea are diagnosed at seasonal and interannual timescales and at different vertical layers, using the state-of-the-art simulations of the Ocean General Circulation Model (OGCM) for Earth Simulator (OFES). Asian monsoon leaves clear seasonal footprints on the eastern Indonesian seas. Consequently, the subsurface waters (around 24.5σ_θ and at ~150 m) in both the Maluku Sea and the Halmahera Sea stem from the South Pacific (SP) during winter monsoon, but during summer monsoon the Maluku Sea is from the North Pacific (NP), and the Halmahera Sea is a mixture of waters originating from the NP and the SP. The monsoon impact decreases with depth, so that in the Maluku Sea, the intermediate water (around 26.8σ_θ and at ~480 m) is always from the northern Banda Sea and the Halmahera Sea water is mainly from the SP in winter and the Banda Sea in summer. The deep waters (around 27.2σ_θ and at ~1 040 m) in both seas are from the SP, with weak seasonal variability. At the interannual timescale, the subsurface water in the Maluku Sea originates from the NP/SP during El Niño/La Niña, while the subsurface water in the Halmahera Sea always originates from the SP. Similar to the seasonal variability, the intermediate water in Maluku Sea mainly comes from the Banda Sea and the Halmahera Sea always originates from the SP. The deep waters in both seas are from the SP. Our findings are helpful for drawing a comprehensive picture of the water properties in the Indonesian seas and will contribute to a better understanding of the ocean-atmosphere interaction over the maritime continent.

Key words: water mass, Indonesian throughflow, monsoon, ENSO, Maluku Sea, Halmahera Sea

Citation: Wang Lu, Zhou Lei, Xie Lingling, Zheng Quanan, Li Qiang, Li Mingming. 2019. Seasonal and interannual variability of water mass sources of Indonesian throughflow in the Maluku Sea and the Halmahera Sea. Acta Oceanologica Sinica, 38(4): 58–71, doi: 10.1007/s13131-019-1413-7

1 Introduction

The Indonesian seas as shown in Fig. 1 are a unique area that connects two major ocean basins (Sprintall et al., 2014). The Indonesian throughflow (ITF) is the only major channel for transporting tropical waters from the Pacific Ocean to the Indian Ocean at low latitudes (Gordon, 2005). It has significant impacts on the ocean circulation and the heat exchange with the atmosphere (Godfrey, 1996). Thus, examining the variation of the ITF and its hydrological properties is important for investigating ocean and climate change.

Generally, there are three main pathways of the ITF (Fig. 1), i.e., the central and dominant pathway through the Makassar Strait with a transport of 9–11.6 Sv (1 Sv=10^6 m^3/s) (Gordon and Fine, 1996; Wajsowicz and Roxana, 1996; Susanto and Gordon, 2005; Pujiana et al., 2009; Gordon et al., 2010), the western pathway through the Luzon Strait, the South China Sea, and the Karimata Strait with a smaller transport of 2–4 Sv (Qu et al., 2005, 2006; Tozuka et al., 2009; Fang et al., 2010; Gordon et al., 2012; Susanto et al., 2012, 2013), and the eastern pathway through the Maluku Sea and the Halmahera Sea (Van Aken et al., 2009). Comparing to the central and western pathways of the ITF, the ITF in the Maluku Sea and the Halmahera Sea is lack of understanding (Wang et al., 2018). The estimated transport varies from 1 to 3 Sv with a quite large uncertainty (Luick and Cresswell, 2001; Talley and Sprintall, 2005; Van Aken et al., 2009). The uncertainty in the eastern pathway is thought to be an important reason for the un-

Foundation item: The GASI Project under contract Nos GASI-IPOVAI-01-02 and GASI-02-SCS-YGST2-02; the National Natural Science Foundation of China under contract Nos 41776034 and 41706025; the Foundation of Guangdong Province for Outstanding Young Teachers in University under contract No. YQ201588.
*Corresponding author, E-mail: llingxie@163.com

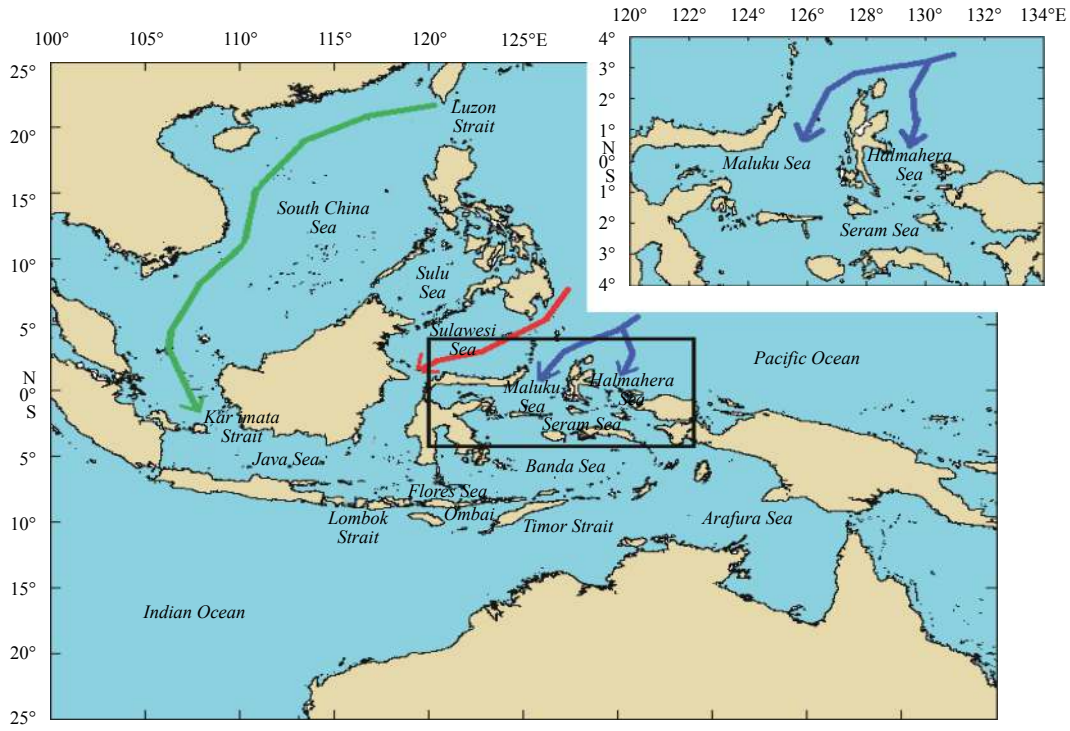

Fig. 1. Topography of Indonesia seas. Green, red and blue lines represent the west, middle and east pathways of the ITF, respectively.

balanced ITF transport. This motivates us to focus on the eastern branch of the ITF, i.e., the Maluku Sea and the Halmahera Sea.

Affected by the Asian-Australian monsoon, the ITF has been found to have a strong seasonal variability in the upper layer. The World Ocean Circulation Experiment (WOCE) and JADE (Hydrodynamics Experiment in Australia) observations show that there is a strong seasonal variability in the sea surface dynamic height, which characterizes the variability of the ITF. Using the moored Acoustic Doppler Current Profiler (ADCP) observations from January 2004 to May 2009 in the Makassar Strait, which is the main pathway of the ITF, Susanto et al. (2012) found that the maximum velocity in the thermocline decreased from –0.8 m/s (minus means southward) during the southeast monsoon to –0.6 m/s during the transition period to the northwest monsoon. Correspondingly, the transport decreased from –13.7 to –9.6 Sv. Interannually, the ITF is affected by the El Niño and South Oscillation (ENSO) events. Meyers (1996) concluded that the ITF weakens during El Niño years and strengthens during La Niña years. The lead-leg correlation coefficients between the Niño3.4 index and the ITF transport from 1984 to 2013 have a maximum value of above –0.5. Based on the ocean model results, the ITF lags the ENSO by 8–9 months. Removing the effects of ENSO by the partial correlation, the Niño3.4 index and the ITF transport has a significant positive correlation (England and Huang, 2005; Liu et al., 2015). The seasonal and interannual variability in the Maluku Sea and the Halmahera Sea with the monsoon and the ENSO, however, remain unclear.

The water mass sources are important for understanding the ITF (Miyama et al., 1995; Godfrey, 1996). The variable vertical structures of temperature-salinity properties and velocities in the Indonesian seas imply different water sources of the ITF at different levels in different seas (Wyrtki, 1961; Miyama et al., 1995; Godfrey, 1996; Susanto and Gordon, 2005). Wang et al. (2018) studied the climatological analysis about the source through the eastern channel of the ITF with World Ocean Atlas 2013 (WOA2013) data. But for the relationship with monsoon and ENSO, there is still no corresponding research. Therefore, this paper focuses on the seasonal and interannual variabilities of water sources of the ITF in the Maluku Sea and the Halmahera Sea, particularly at the subsurface, intermediate and deep layers.

The rest of the paper in organized as follows. The data and the methods are described in Section 2. Sections 3 and 4 show the seasonal and interannual variabilities of the water mass sources, respectively. A summary of the results is given in the last section.

2 Data and methods

2.1 *OFES data*

The high-resolution temperature, salinity and velocity data from the Ocean General Circulation Model (OGCM) for Earth Simulator (OFES) are used in this study. OFES is based on the Geophysical Fluid Dynamic Laboratory's Modular Ocean Model (MOM3). The model domain covers from 75°S to 75°N, with horizontal resolution of (1/10)°. In vertical, there are totally 54 layers from surface to the maximum 6 065 m, with depth interval varying from 5 to 330 m (Sasaki et al., 2008). The climatologically monthly data in February and August are used for seasonal variability analysis. For the interannual variability, monthly-mean data corresponding to the ENSO events during the period from January 1997 to December 2013 are selected, which include three El Niño events and three La Niña events, respectively.

In order to validate the OFES data, the WOA2013 data provided by National Oceanographic Data Center (http://apdrc.soest.hawaii.edu/las/v6/dataset?var=15101) are used for comparison. Figures 2a and b show the vertical distribution of the climatological salinity along 160.125°E in the Pacific from the OFES and WOA2013, respectively. One can see that the vertical distributions of salinity against depth from the two data are very similar. There are high-salinity waters with S>34.9 around 24.5σ_θ at depths of 100–300 m in the subsurface layer on both sides of the

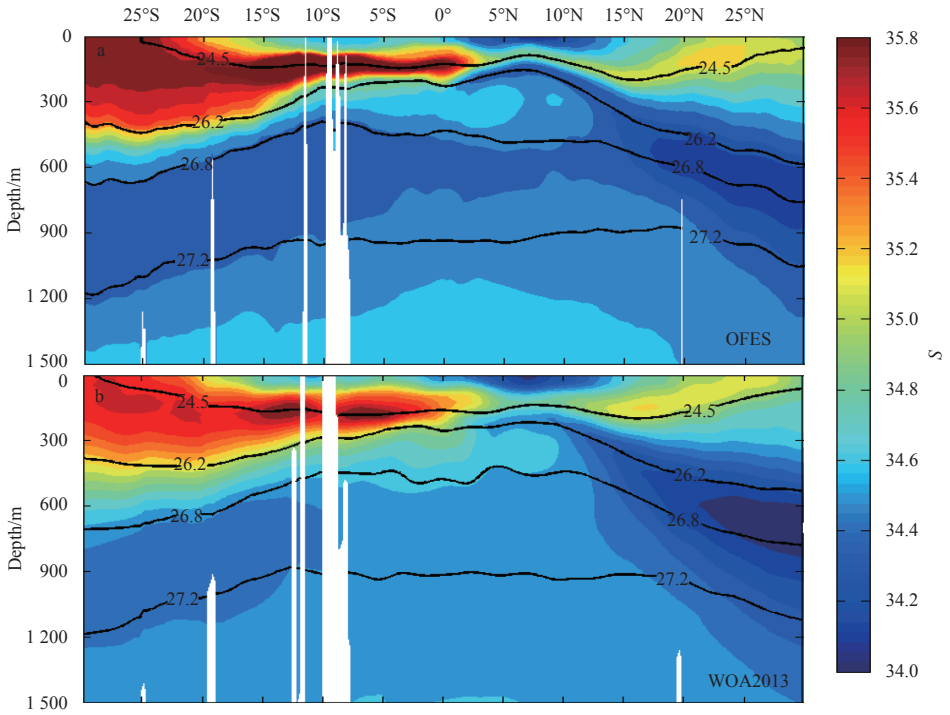

Fig. 2. Distribution of salinity against depth along Section 160.125°E in the upper 1 500 m in the Pacific. a. OFES data and b. WOA2013 data. The black lines represent the isopycnals of potential density.

equator, which are associated with the North Pacific Tropic Water (NPTW) and the South Pacific Tropic Water (SPTW), respectively (Qu et al., 2000; Xie et al., 2009; Wei et al., 2016a). Comparing to the SPTW, the characteristic density and salinity of the NPTW is a little lower by 0.5 kg/m^3 and 0.4. Below the high-salinity waters, low-salinity waters with S<34.4 around 26.8σ_θ appear in the intermediate layer at about 500–900 m in the NP, where the North Pacific intermediate water (NPIW) dominates. In the SP, the low-salinity water of Antarctic Intermediate Water (AAIW) has characteristic salinity and density a little higher than that of the NPIW by 0.1 kg/m^3 and 0.2. In the deep layer, the salinity increases at depths below 27.2σ_θ. Though there are some systematically bias from the WOA data, the relative variation of the salinity of the OFES data can be used to trace water masses.

2.2 *Sea surface wind and topography data*

The sea surface wind data are satellite products download from the Asia-Pacific Data-Research Center (APDRC) (http://apdrc.soest.hawaii.edu/data/data.php?discipline_index=2). The topography data are the ETOPO1 data from the National Centers for Environmental Information (https://www.ngdc.noaa.gov/mgg/global/global.html).

2.3 *Niño3.4 index*

The Niño3.4 index, i.e., the average of the sea surface temperature (SST) anomalies over the region 5°N–5°S and 170°–120°W, is used to identify the El Niño and La Niña events. The data are downloaded from National Oceanic and Atmospheric Administration (NOAA) (http://apdrc.soest.hawaii.edu/las/v6/constrain?var=951). It is defined as an El Niño or La Niña event if the 3-month running-average of the Niño3.4 index exceeds +0.5°C or –0.5°C for at least 5 consecutive months (Hanley et al., 2003). According to the definition, we found three El Niño events and three La Niña events during the period from 1997 to 2013. Details are shown in Section 4.

2.4 *Water masses and analysis methods*

As shown in Fig. 2, there are two different kinds of water masses in the NP and the SP, i.e., the high-salinity waters of NPTW and SPTW around 24.5σ_θ, and the low-salinity water NPIW and AAIW around 26.8σ_θ. Figure 3a further shows the relationship of the potential temperature versus salinity, i.e., the θ-S diagram, in the NP (blue dots) and the SP (red dots). One can see that the striking reversed S shape of the θ-S diagrams in the NP and the SP, due to the high-salinity water of NPTW (S>35.0) and SPTW (S>35.4) and the low-salinity water of NPIW (S<34.4) and AAIW (S>34.6). The characteristic densities of the SP waters are larger than that in the NP. In the two study seas as shown in Fig. 3b, the reversed S shape is not as evident as that in the NP and the SP, especially in the Maluku Sea (black dots). The characteristic salinities are relatively lower in the subsurface water and higher in the intermediate water than that in the Pacific. The characteristic density of the subsurface high-salinity water in the two seas are similar to that in the Pacific, i.e., about 24.5σ_θ, while characteristic density of the low-salinity water in the two seas are close to 27.2σ_θ in the deep layer.

We use the water property distribution on isopycnal surface, combining with velocity distribution, to trace the water masses. Such methods have been widely used in previous studies (Qu et al., 1999; Zhang et al., 2008; Xie et al., 2009). Considering the typical warm-salty and cold-fresh water masses in the study area, shown in Figs 2 and 3, in the following analysis, characteristic densities of 24.5σ_θ and 26.8σ_θ are selected to represent the subsurface water and the intermediate waters. The values are a little different from 25.0σ_θ and 26.7σ_θ used by Qu et al. (2000) and Wei et al. (2016a) in the SCS. It is reasonable if considering the different water mass sources and water mass transformation. In fact, both the above values are in the density range of the same water

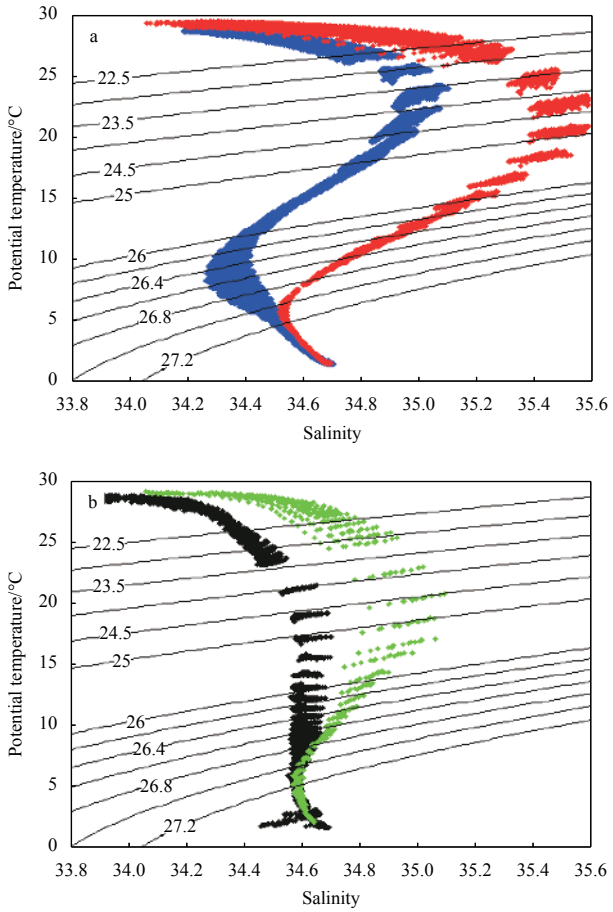

Fig. 3. θ-S diagram in the study areas. a. The NP (blue dots) and the SP (red dots), and b. the Maluku Sea (black dots) and the Halmahera Sea (green dots).

mass. The different choice of characteristic density has little effect on the following water mass analysis. Between the subsurface and intermediate layers, we also chose a density of 26.2σ_θ for the transition layer analysis. In the deep layer, the density of 27.2σ_θ is selected considering the low-salinity water masses in the Maluku Sea and the Halmahera Sea as shown in Fig. 3b.

3 Seasonal variability of water mass sources

The study area is located in the low latitudes near the equator, and affected by the Asian-Australian monsoon. There is northeasterly wind during the winter monsoon from December to April of the next year, and southeasterly wind during the summer monsoon from May to October. As shown in Fig. 4, February and August are chosen to be the representative months of the winter monsoon and the summer monsoon, respectively. The water mass sources of the Maluku Sea and the Halmahera Sea are investigated according to the variation of the depths and salinities on characteristic isopycnal surfaces.

3.1 *Subsurface water around 24.5σ_θ*

Figures 5a and b show the horizontal distribution of isopycnal depth of 24.5σ_θ in February and August, respectively. One can see that the depths of 24.5σ_θ are zonally distributed in the Pacific, with largest values of 150–200 m at latitudes of 15°–20°N, smallest values of 50–100 m at 5°–10°N, and relatively larger values of 100–150 m at 5°S–5°N near equator. Comparing the values in February (Fig. 5a), the isopycnal of 24.5σ_θ deepens in August during the summer monsoon in both the north and south Pacific. For the two study seas, the depths in the Maluku Sea are about 120 m and have little change from winter to summer, while the depths in the Halmahera Sea increase from 100 m in winter to 120 m in summer.

Figure 5c shows the salinity distribution on isopycnal surface of 24.5σ_θ in February. One can see that high salinity water (S>35.7) in the SP associated with the SPTW expands significantly northward along the coast of New Guinea, crosses the equator and forms a strong salinity front at about 4°N with the relatively low-salinity water (S<35) from the NP. The salinity in the Halmahera Sea is larger than 35.5, which is higher than that of the NP water by 0.5 but quite similar to the SP water. On the other hand, the salinity in the southern Maluku Sea is about 35.5, which is close to that in the Halmahera Sea. It seems that the subsurface water of the Halmahera Sea and the Maluku Sea come from the SP. In August, as shown in Fig. 5d, the northward SPTW has a higher salinity (S>35.9) and closely hugs the coast than that in February. In the north of equator, a cloud of high-salinity water (S>35.5) separates from the coast and circles in the northwest of the Halmahera Island, indicating of the Halmahera Eddy. The salinity in the Halmahera Sea is about 35.9, which is higher than that of the NP water by 0.9 but similar to the SP water. It is clear that in the summer monsoon, the subsurface water of the Halmahera Sea comes from the SP. However, in the Maluku Sea, the salinity is lower than 35.2, which is closer to the NP water rather than the SP water.

The velocities in the subsurface layer are shown in Fig. 6. One can see that during the winter monsoon in February, strong anticyclonic circulation dominates in the equatorial Pacific with the

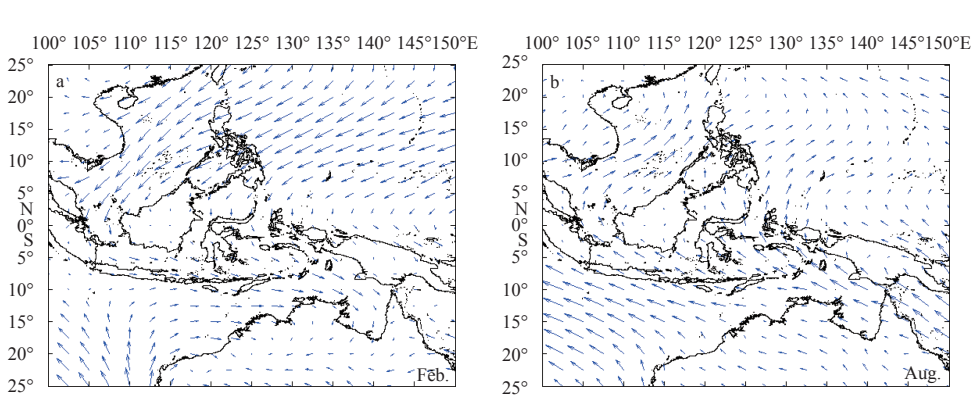

Fig. 4. Satellite-derived surface wind vectors in the study area in February (a) and August (b).

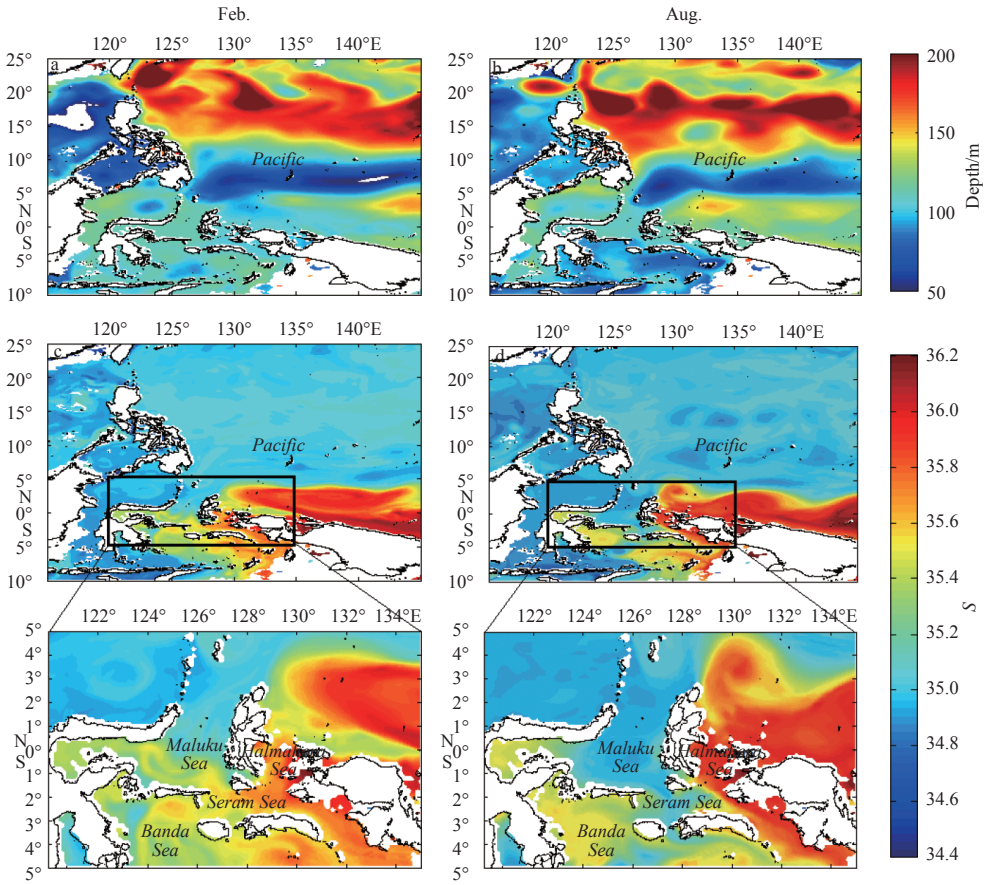

Fig. 5. Distribution of depth (a, b) and salinity (c, d) on isopycnal surface of 24.5σ_θ in February (a, c) and August (b, d). The bottom panels are magnification of the black box in the row above.

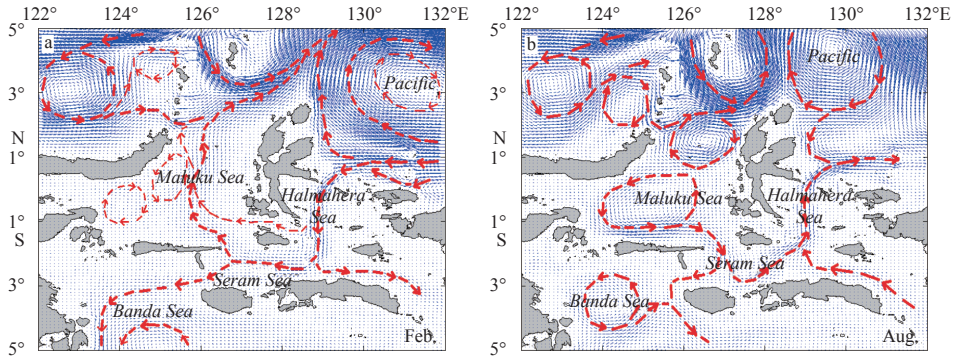

Fig. 6. The currents on the isopycnal surface of 24.5σ_θ in February (a) and August (b). Red arrows represent the flow directions.

northwestward New Guinea Coastal Current (NGCC) crossing the equator from SP and the eastward Northern Equatorial Countercurrent (NECC) north of 5°N (Fig. 6a). In the studied Maluku Sea, the weak currents mainly flow northward. It has two inflow pathways in the south, one is the Lifamatora passage near the Banda Arc and the other is the narrow strait between the Maluku Sea and the Halmahera Sea. The two inflows merge in the Maluku Sea, flow northward along the central Maluku Sea, and turn northeastward to the Pacific within the NECC. At the same time, in the west of the Maluku Sea, there are two circulations, one is cyclonic and the other is anticyclonic. In the Halmahera Sea, the main flow is southward. The northwestward NGCC branches into the Halmahera Sea as flowing along the islands coast. It is this branch carrying the SP water into the Halmahera Sea, passing through the Halmahera Sea, and further turning westward into the Maluku Sea and eastward into the Seram Sea. The velocity field in February supports the isopycnal analysis results that the water mass in the Maluku Sea and the Halmahera Sea are both from the SP.

During the summer monsoon in August (Fig. 6b), the circulation in the Maluku Sea reverses to be anticyclonic in the north and cyclonic in the south. In the northern mouth of the Maluku Sea, the southward current from the Mindanao coast and the eastward outflow from the Sulawesi Sea are mixed. Most of the mixed water goes eastward as the Mindanao Eddy and the NECC, while a small part goes southward along the eastern boundary of

Maluku sea and then westward in composition of the anticyclonic circulation. Meanwhile, the westward flow also separates southward at the western boundary of the Maluku Sea to form the cyclonic circulation in the southern part of the Maluku Sea. It confirms that the subsurface water in the Maluku Sea comes from the NP, consistent with the salinity analysis. In the Halmahera Sea, the flow is mainly northward. It is merged by the current leaving out of the Maluku Sea with the NP water, and the flow from the southern Seram Sea with the SP water. Combining with the salinity distribution in Fig. 5d, the high-salinity SP dominates the mixed water in the Halmahera Sea in August.

As shown above, the seasonal variability of the water sources in the two study seas are different. The subsurface water of the Maluku Sea is mainly from the SP during winter but from the NP during summer. The Halmahera Sea water is from the SP during winter but a mixture of the NP and SP water during summer.

3.2 *Transition layer around 26.2σ_θ*

On the surface of 26.2σ_θ (Figs 7a and b), the depth distribution is similar to that in the subsurface layer, except that the central latitudes of the zonal bands shift northward. The deepest value of 500 m appears to the north of 20°N, and the shallowest values of 200 m at about 8°N. In the Maluku Sea and the Halmahera Sea, the depths are about 250 m. Different from the variability in the subsurface layer, the depths of 26.2σ_θ in August is shallower than that in February. For the salinity distribution (Figs 7c and d), there is a low salinity of about 34.4 in the Maluku Sea both in winter and summer, indicating of the NP water source. In the Halmahera Sea, the salinity is about 34.7 in winter, close to the SP water, but decreases to about 34.4 in summer, which is close to the NP water.

The circulation currents in this layer are shown in Fig. 8. During winter monsoon, there is an anticyclonic circulation in the Maluku Sea. In the north Maluku Sea, the outflow from the Sulawesi Sea merges into the anticyclonic circulation and flows to the southern Maluku Sea. Part of it flows further southward, and leaves the Maluku Sea from the Lifamatora passage. In the Halmahera Sea, the flow enters from the northern strait and goes out from the southern strait. The circulation indicates that the Maluku Sea water is mainly from the NP and the Halmahera Sea water is mainly from the SP during winter monsoon. In summer, the Maluku Sea water is still from the NP as the merged flow from the Sulawesi Sea and the Mindanao coast. The flow in the Halmahera Sea reverses to be northward in summer, which comes from the Maluku Sea through the southern strait, and leaves out to the Pacific through the northern strait. Both the water sources in the two study seas are from the NP during the summer monsoon.

Therefore, it can be concluded that on the transitional layer, the Maluku Sea water is from the NP during both winter and summer monsoon, but the Halmahera Sea water is from the SP during winter and the NP during summer.

3.3 *Intermediate water around 26.8σ_θ*

Figure 9 shows the depth and salinity distribution in the intermediate layer around 26.8σ_θ. One can see that the banded depths are larger than 800 m at latitudes north of 25°N, and less than 500 m

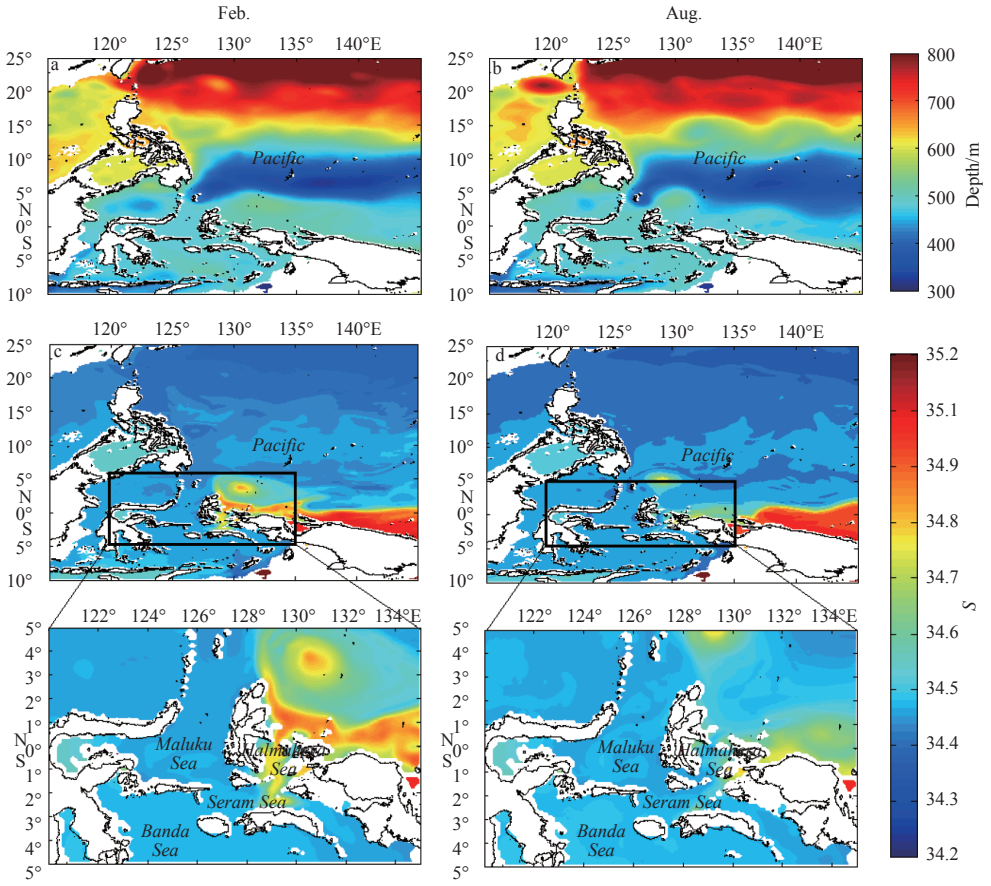

Fig. 7. Distribution of depth (a, b) and salinity (c, d) on isopycnal surface of 26.2σ_θ in February (a, c) and August (b, d). The bottom panels are magnification of the black box in the row above.

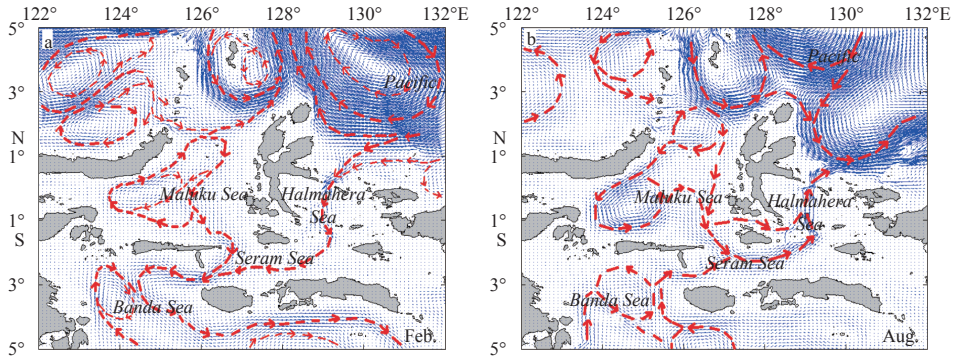

Fig. 8. The currents on the isopycnal surface of 26.2σ_θ in February (a) and August (b). Red arrows represent the flow directions.

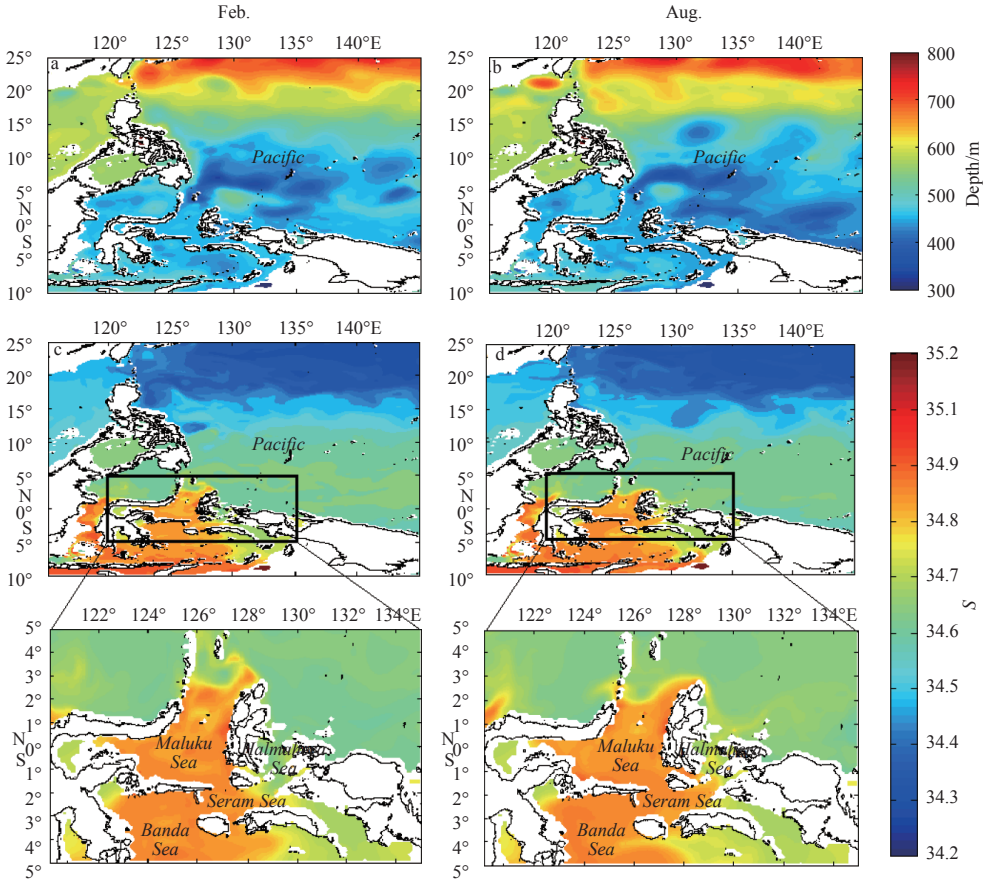

Fig. 9. Distribution of depth (a, b) and salinity (c, d) on isopycnal surface of 26.8σ_θ in February (a, c) and August (b, d). The bottom panels are magnification of the black box in the row above.

in the south of 10°N in both the NP and the SP near the equator. In the Halmahera Sea and the Maluku Sea, the isopycnal depths are about 450 m. The salinity distribution is similar to that of depth. The salinity less than 34.3 dominates the area north of 15°N, and relatively high salinity of about 34.5 appears in the south of 10°N. In the Maluku Sea, the salinity of 34.7 is dramatically higher than that in the Pacific, but close to the that in the southern Seram Sea and the Banda Sea. It seems that the Maluku intermediate water comes from the Banda Sea. The seasonal variation is not remarkable. It may agree with the result by Van Aken et al. (2009), who suggested that the flow through the eastern Indonesian basins had weak seasonal variability at depths below 260 m. However, in the Halmahera Sea, the winter salinity differs from that in summer. It might come from the Pacific with a salinity of 34.5 in winter, and from the Saran Sea with higher salinity of 36.6 in summer.

The circulation can further explain the water source of the study seas in the intermediate layer. As shown in Fig. 10, the main flow in the Maluku Sea is mostly northward in both winter and summer. It origins from the north Banda Sea, passes the Saran Sea, and enters the Maluku Sea through the Lifamatora passage. In the Maluku Sea, it circles anticyclonically and finally goes out through the northern mouth to the Pacific. For the Halmahera Sea, the flow is southward in winter and reverses to be northward in summer. In winter, the flow is from the SP, enters the Halmahera Sea and further turns southward to the

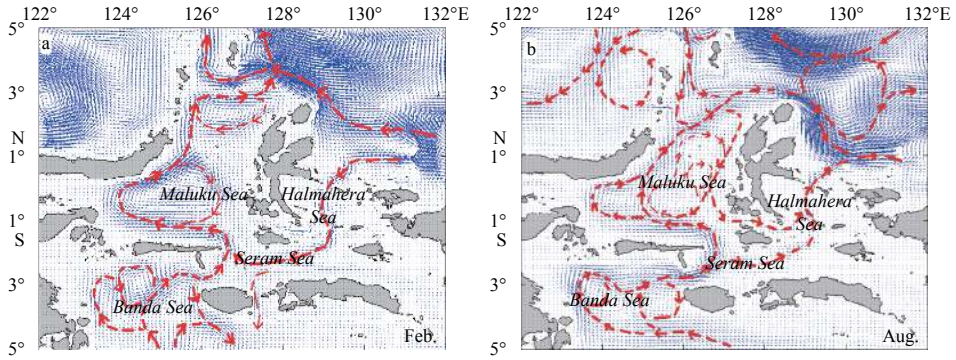

Fig. 10. The currents on the isopycnal surface of 26.8σ_θ in February (a) and August (b). Red arrows represent the flow directions.

Saran Sea. In summer, the flow is from the Saran Sea, passes through the Halmahera Sea and flows into the SP.

Thus, in the intermediate layer, the Maluku Sea water is mainly from the Banda Sea in both winter and summer, while the Halmahera Sea water is mainly from the SP in winter and Banda Sea in summer.

3.4 *Deep water around 27.2σ_θ*

On the surface of 27.2σ_θ in the deep layer (Fig. 11), the distribution of isopycnal depths is different from the upper layer. The band of the shallow depths of 800–850 m shift northward to 10°–15°N and the depths in the south of 5°N are relative deeper being about 950 m in February and about 900 m in August. The depths around 930 m remain unchanged in the Maluku Sea, which are close to those in the Pacific. The Halmahera Sea is isolated by shallow topography in this layer. The distribution of salinity has almost the same pattern in winter and summer, and values are quite uniform as 34.5 in the western NP and SP. The salinity in the Maluku Sea is also about 34.5, which is close to that in the Pacific. In the isolated Halmahera Sea, the salinity is about 34.6, higher than the surrounding area.

Figure 12 shows the currents in the deep layer. One can see that the velocity in the isolated Halmahera Sea basin is quite weak, while a cyclonic flow dominates in the Maluku Sea in both winter and summer. In winter, the northward flow from SP crosses the Mindanao-Halmahera waterway and enters the

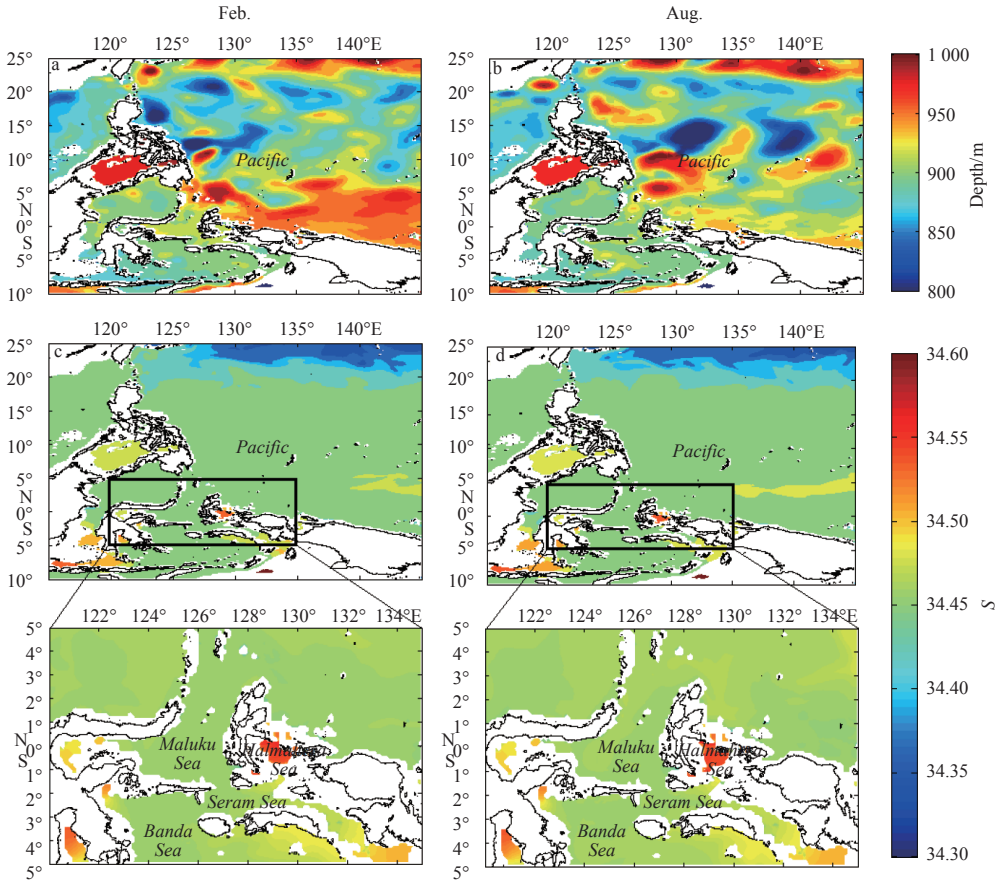

Fig. 11. Distribution of depth (a, b) and salinity (c, d) on isopycnal surface of 27.2σ_θ in February (a, c) and August (b, d). The bottom panels are magnification of the black box in the row above.

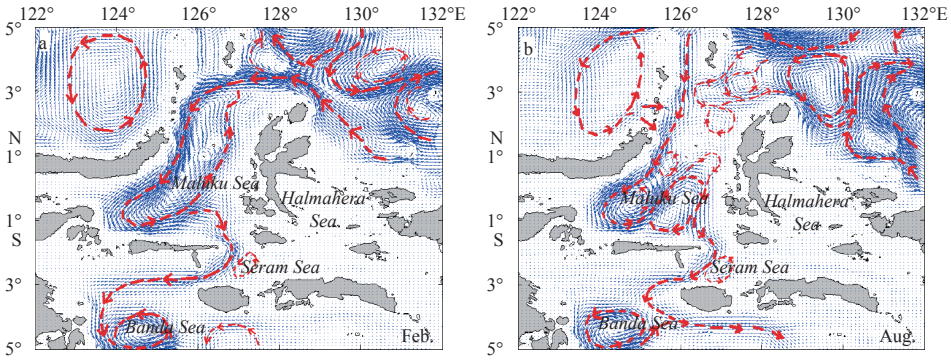

Fig. 12. The currents on the isopycnal surface of 27.2σ_θ in February (a) and August (b). Red arrows represent the flow directions.

Maluku Sea. It cyclonically circulates in the Maluku Sea with a branch leaves out from the Lifamatora passage. It can be concluded that the water source of the Maluku Sea is always from the SP in the deep layer with a less seasonal variability.

4 Variability of water sources during ENSO

Previous studies have shown that the ITF is not locally forced, but rather forced by large scale winds in the Pacific (Godfrey, 1989; Meyers, 1996; Du and Qu, 2010; Tozuka et al., 2009; Liu et al., 2015). In this section, the interannual variability of the water sources in the eastern path of the ITF related to the ENSO is analyzed. As shown in Fig. 13, there are three El Niño events and three La Niña events during the period from 1997 to 2013. The El Niño and La Niña months are extracted. There are totally 32 months from May 1997 to May 1998, May 2002 to March 2003, and June 2009 to April 2010 for El Niño event, and 26 months from July 1998 to May 2000, September 2007 to May 2008, and July 2010 to March 2011 for La Niña event.

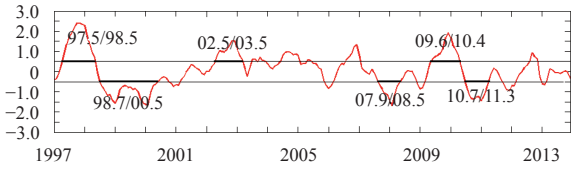

Fig. 13. Niño3.4 index from January 1997 to December 2013. The numbers in the figure indicate year and month.

To remove the seasonal variability, the mean values of the all 32/26 El Niño/La Niña months are not directly averaged. We first average the values in the same month, e.g., all the values in May in El Niño event are averaged. Then, the monthly mean values in different months in the El Niño/La Niña event are averaged to obtain the final values representing the El Niño/La Niña event. Properties with significant variation, such as the isopycnal depths on 24.5σ_θ, 26.8σ_θ and 27.2σ_θ and the velocities at the corresponding depths, are used to investigate the variation of water sources during the El Niño and La Niña periods.

4.1 *Subsurface layer around 24.5σ_θ*

In the subsurface layer (around 24.5σ_θ) shown in Fig. 14, the depths in El Niño are obviously shallower than those in La Niña in the ITF source area south of 10°N. During the El Niño period (Fig. 14a), the isopycnal depths of 24.5σ_θ are shallower than 60 m at 5°–10°N in the NP and deeper than 120 m at 5°S–0° in the SP. The shallow depths in the NP extend southward along the Mindanao coast, and branches into the Sulawesi Sea and the Maluku Sea. In the SP, the deeper depths of 110 m show a weaker northward extension along the New Guinea coast and are restricted east of 140°E. In the study seas, the depths are shallower than 100 m, indicating the influence of the NP water. During La Niña (Fig. 14b), the isopycnal depths are larger than 130 m in the SP, and extend further northward to the Halmahera Island at 130°E. The depths in the Maluku Sea and Halmahera Sea increase to about 120 m, which are probably influenced by the SP water.

Figure 14c show the currents of the interested area in the subsurface layer during the El Niño period. One can see that the flows in the Maluku Sea and the Halmahera Sea are mainly southward. In the Maluku Sea, the flow comes from the Sulawesi Sea, goes through the basin, and turns eastward at the southern Maluku Sea with a branch into the Halmahera Sea. In the Halmahera Sea, the southward flow mainly comes from the SP, and combines with that from the Maluku Sea. Thus, in El Niño, the subsurface water source is from the NP in the Maluku Sea, while the SP may dominate in the Halmahera Sea.

During the La Niña period (Fig. 14d), the flow into the Halmahera Sea from the SP strengths as the deeper depth shown in Fig. 14b. A small part of the flow enters the Maluku Sea through the narrow straits between the two seas, and the other leaves out into the Seram Sea as westward flow. The westward flow in the Seram Sea also has northward branching into the Maluku Sea through the Lifamatora passage. The flow into the Maluku Sea circulates in the basin and finally leaves into the Pacific. It is clear that the subsurface water of the Halmahera Sea and the Maluku Sea are mainly from the SP during the La Niña period.

Comparing the two study seas, one can see that the subsurface water sources in the Maluku Sea significantly changes from the NP in El Niño to the SP in La Niña, while the Halmahera Sea water is mainly from SP both in the El Niño and La Niña periods. The Student's *t*-test result further indicates that the variation between the El Niño and La Niña are significant in most equatorial Pacific and Indonesian seas as shown in Fig. 15a. The depth differences are larger than 40 m in the convergence zone between 0° and 5°N, which is the source area of the Maluku Sea and the Halmahera Sea. This distinction confirms the influence of ENSO on the subsurface layer in the study area.

4.2 *Intermediate layer around 26.8σ_θ*

In the intermediate layer, isopycnal depths on 26.8σ_θ in El Niño and La Niña are shown in Figs 16a and b. One can see that the depths in the two study seas deepen a little from about 400 m in El Niño to 450 m in La Niña, which is a similar trend to that in

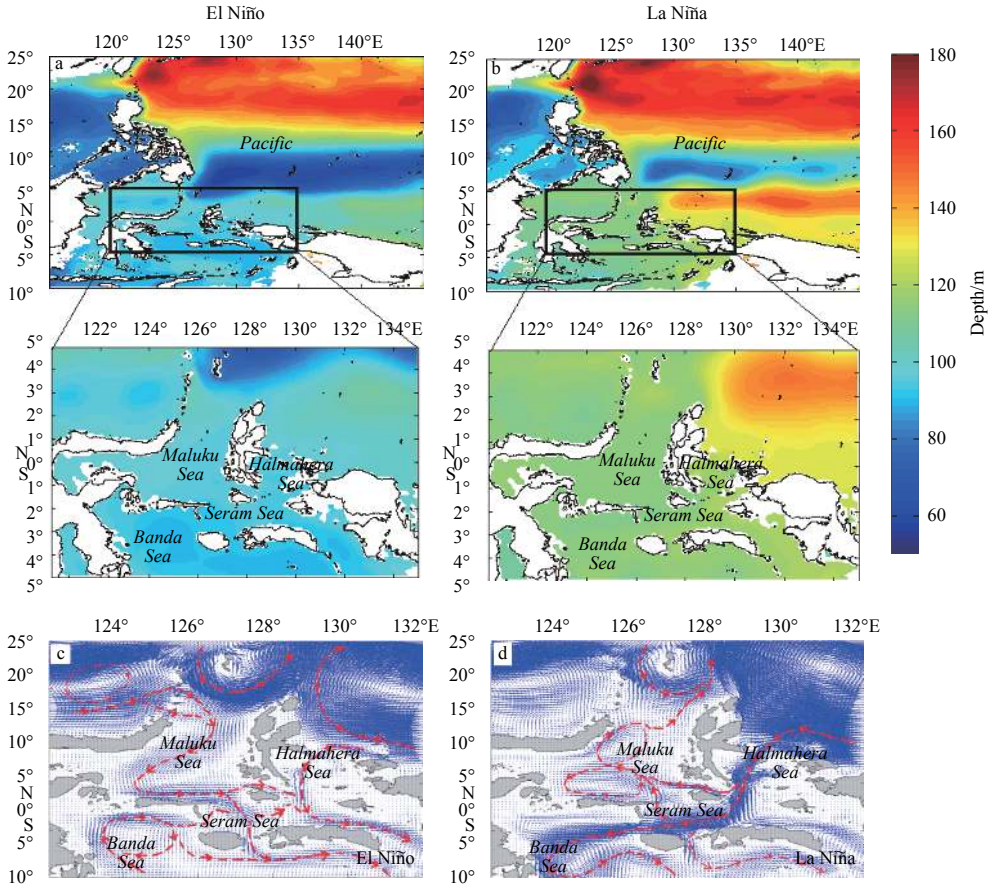

Fig. 14. Distribution of depth (a, b) and velocity (c, d) on isopycnal surface of 24.5σ_θ in El Niño (a, c) and La Niña (b, d).

the upper layer. However, it is different from the subsurface layer, in which the isopycnal depths in the SP are shallower than those in the NP. The intermediate waters in the Maluku Sea and the Halmahera Sea seem to be more related to that in the SP.

Figures 16c and d show the currents in the intermediate layer in El Niño and La Niña. One can see that the northward undercurrent in the SP flows far northward over the equator to the Mindanao coast during the El Niño. It splits into the Halmahera Sea near equator and affects the northern Maluku Sea near the Mindanao Island. Definitely, the Halmahera Sea intermediate water comes from the SP in El Niño. In the Maluku Sea, there is also evident northward flow from the northern Banda Sea. Part of the SP from the Halmahera Sea and Seram Sea may also go into the Maluku Sea from the Lifamatora passage. During the La Niña period, the northward undercurrent in the SP weakens. It turns eastward on the east of Halmahera Island without reaching the Maluku Sea. The branch into the Halmahera Sea also weakens, while the northward flow from the Banda Sea in the Maluku Sea strengthens. Though the currents vary in some extent, the main water mass sources of the Maluku Sea and the Halmahera Sea are from the Banda Sea and the SP, respectively, in both El Niño and La Niña.

4.3 *Deep layer around 27.2σ_θ*

In the deep layer (Figs 17a and b), the isopycnal depths of 27.2σ_θ are less than 900 m in the western boundary of the NP and larger than 1 000 m in the SP. Comparing to the El Niño, the depths south of 10°N increase in La Niña. In the Maluku Sea, the depths are about 950 m and increase in La Niña as the increase in the SP. Figures 17c and d show the currents in the deep layer which are almost the same in the El Niño and La Niña. The flow from the SP expands northwestward, crosses the equator and branches into the Maluku Sea. The flow into the Maluku Sea goes southward along the west boundary, turns eastward along the south boundary, and leaves out to the Seram Sea and the Banda Sea. Both the depth and current distributions indicate that the water source of the Maluku Sea in the deep layer is always from the SP in both El Niño and La Niña periods. The depths in the Halmahera Sea are shallower than that in the Maluku Sea due to the isolation. The flow is also quite weak. The deep water there might be shallow water overflows from the upper layer in the SP.

Comparing to the subsurface layer, the intermediate and deep water sources in the Maluku Sea and the Halmahera Sea have no significant variability. The significant difference area between El Niño and La Niña also dramatically shrinks on 26.8σ_θ and 27.2σ_θ in the intermediate and deep layers as shown in Figs 15c and d. The impacts of ENSO should be mainly concentrated in the upper and subsurface layer, with little effect in the intermediate and deeper layers.

5 Summary and discussion

As the key process in the tropic oceans and the global ocean circulation, the ITF in the Indonesian seas has attracted many attentions of researchers. However, much uncertainties are still remained due to the limited knowledge of the ITF in its eastern pathway through the Maluku Sea and the Halmahera Sea (i.e., Wang et al., 2018), especially when considering the vertical variation in different depth layers (Susanto and Gordon, 2005; Zhang

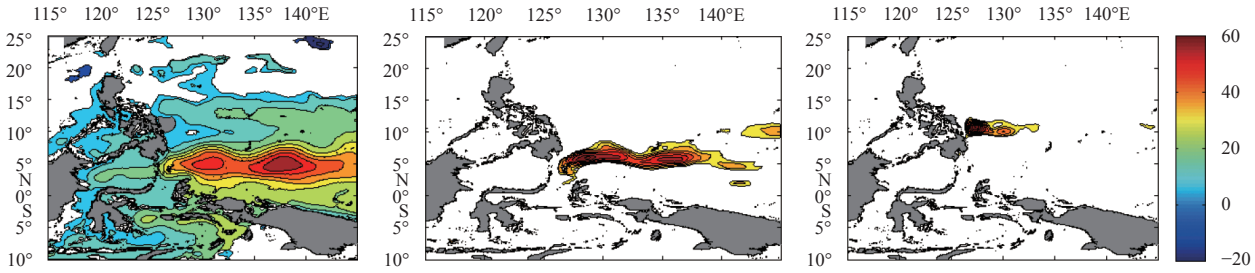

Fig. 15. *T*-test between El Niño and La Niña on 24.5σ_θ (a), 26.8σ_θ (b) and 27.2σ_θ (c). The null region indicates that it does not pass the significance test, and the contour region indicates the area with the confidence level over 0.95. The contours represent the depth difference between that in El Niño and La Niña.

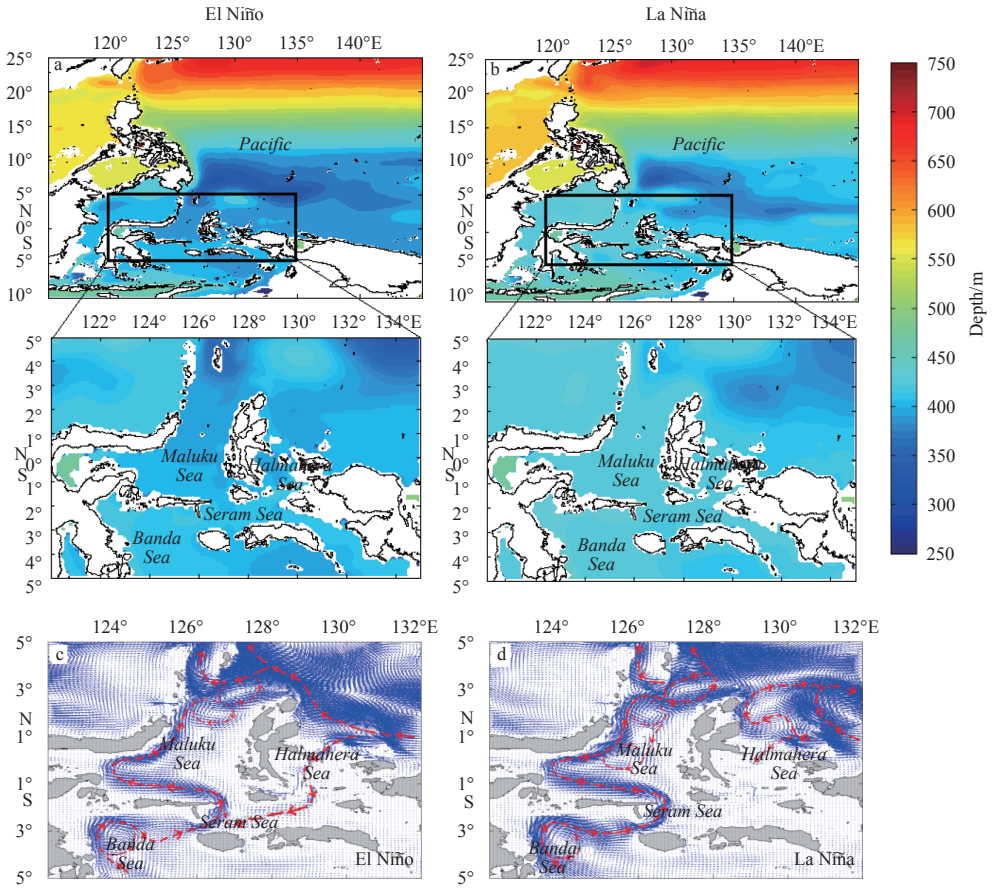

Fig. 16. Distribution of depth (a, b) and velocity (c, d) on isopycnal surface of 26.8σ_θ in El Niño (a, c) and La Niña (b, d).

et al., 2008) and the seasonal and interannual variability at different time scales (Zhao et al., 2015; Yuan et al., 2017).

Previous studies suggest that the ITF in its western pathway through the Luzon Strait and the SCS has a sandwich or four-layer structure in vertical, i.e., westward flow in the upper (surface and subsurface layers) and deeper layers, and eastward flow in the intermediate layer (Tian et al., 2006; Wei et al., 2016b). At the two eastern basins, few studies focused on the vertical structure of the ITF in the Maluku Sea and the Halmahera Sea due to data limit (Wang et al., 2018). Using the Simple Ocean Data Assimilation (SODA) product, Du and Qu (2010) found that the annual mean surface flow is southward, and decreases gradually from the surface to about 400 m. They also found that the surface and subsurface flow changes from southward in summer to northward in winter under the influence of seasonally reversed monsoons. Other results based on SODA data further implies that the eastern pathway is of major importance to the ITF interannual variation, which is related to the ENSO events (Murray and Arief, 1988; Arief and Murray, 1996; Sprintall, 2009). During the El Niño year, northward current anomalies occur in the subsurface layer in the eastern Indonesian basins, flow toward the Pacific, and enhance the NECC (Godfrey, 1989; Wajsowicz, 1993). Since the SODA data cannot well reproduce the velocity profile in the narrow strait because of low resolution (Van Aken et al., 2009), a higher resolution model, like the OFES, is necessary to address the structure and variation of the ITF in its east pathway.

In this study, the OFES data with horizontal resolution of (1/10)° are used to investigate the water sources of the Maluku

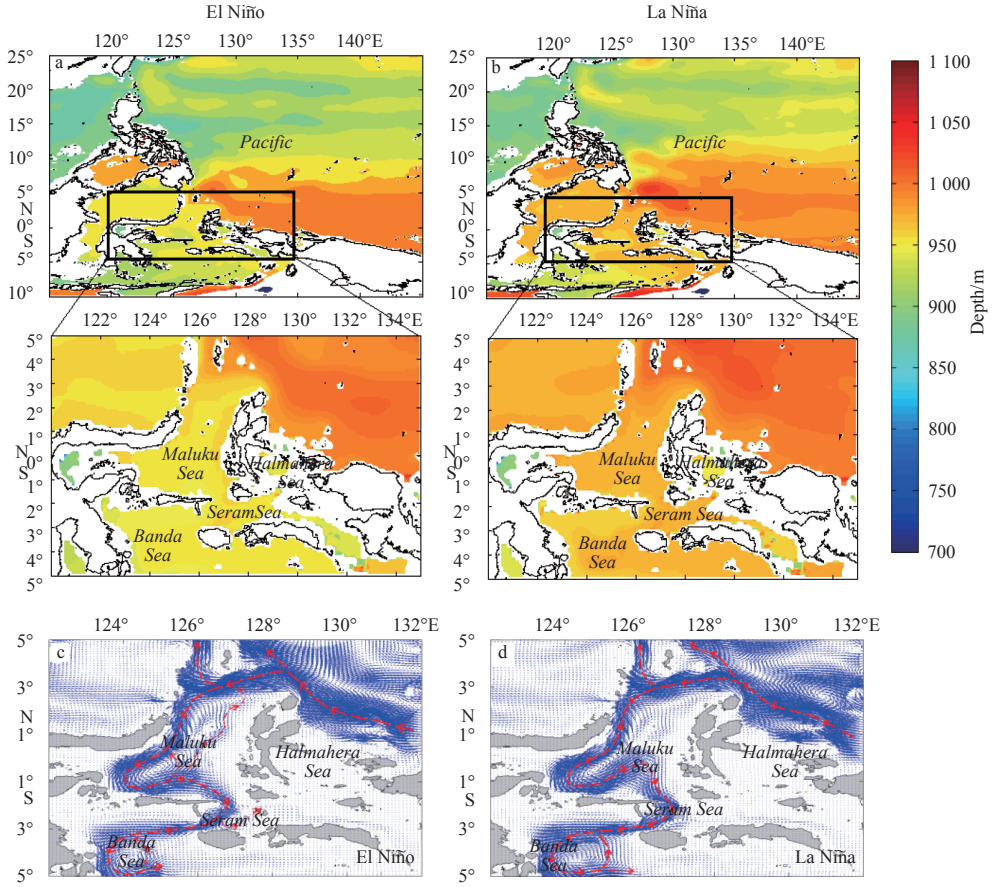

Fig. 17. Distribution of depth (a, b) and velocity (c, d) on isopycnal surface of 27.2σ_θ in El Niño (a, c) and La Niña (b, d).

Sea and the Halmahera Sea. The results are summarized in Table 1. One can see that in the subsurface, the source of Maluku Sea is mainly from the SP during the winter monsoon, but from the NP during the summer monsoon. The Halmahera Sea water is from the SP during the winter monsoon, but is a mixture of waters originating from the NP and the SP during the summer monsoon. In the intermediate layer, the source of the Maluku Sea water is mainly from the Banda Sea both in winter and summer, and the Halmahera Sea water is mainly from the SP in winter and the Banda Sea in summer. Down to the deep layer, the Halmahera Sea water is isolated by the topography. The Maluku Sea water is mainly from the SP both in winter and summer monsoon.

On the interannual time scale, the variation of the ITF in the central pathway has been found to be opposite to that in the western pathway, i.e., the SCS throughflow (SCSIF) in the ENSO events (Liu et al., 2006; Zhao et al., 2015; Wei et al., 2016b). Gordon et al. (2012) pointed out that the Kuroshio water entering the SCS increased during El Niño period. The remote ENSO signals entering the SCS were transferred to the Makassar Strait, and then blocked the MC branch from the Sulawesi Sea into the Indonesian Sea. Should the blocked NP water go through the eastern source region, i.e., the Halmahera Sea and the Maluku Sea, into the ITF? Qu et al. (2006) show that in the La Niña year, fewer Kuroshio waters enter the SCS, resulting in the MC smoothly flowing to the Sulawesi Sea. Would the SP water reach the Maluku Sea and Halmahera Sea at this time? There is no previous observation or study about these questions. Our result, however, gives the answer.

As listed in Table 1, in the subsurface layer, the NP water enters into the Maluku Sea and the SP dominates the Halmahera Sea in El Niño. During the La Niña period, the SP water intensified northward as the NP water retreated, and the SP water crossed the north area of the Halmahera Sea into the ITF through the Maluku Sea and the Halmahera Sea. In the intermediate and deep layers, however, the Maluku Sea water is mainly from the north Banda Sea and the SP both in El Niño and La Niña. The Halmahera Sea water is always from the SP and isolated in the deep layer. ENSO has no discernable influences on the deeper water sources in the study seas.

Both the seasonal and ENSO phases modify the ITF mainly by

Table 1. Variation of water mass sources in three layers in the Maluku Sea and Halmahera Sea

	Subsurface water around 24.5σ_θ		Intermediate water around 26.8 σ_θ		Deep wateraround 27.2σ_θ	
	Maluku Sea	Halmahera Sea	Maluku Sea	Halmahera Sea	Maluku Sea	Halmahera Sea
Winter	SP	SP	Banda Sea	SP	SP	
Summer	NP	mix water of SP and NP	Banda Sea	Banda Sea	SP	
El Niño	NP	SP	Banda Sea	SP	SP	
La Niña	SP	SP	Banda Sea	SP	SP	

changing the circulation and isopycnal surface depth of the West Pacific. Although the time scales are different, the consequences and mechanisms are similar. In this study, we only focus on the source of the Maluku Sea and the Halmahera Sea. Other properties, such as the transport volume, heat flux and freshwater flux, are also important. However, similar diagnoses have to be deferred due to the availability and quality of data and reanalysis products.

References

Arief D, Murray S P. 1996. Low-frequency fluctuations in the Indonesian throughflow through Lombok Strait. Journal of Geophysical Research: Oceans, 101(C5): 12455–12464, doi: 10.1029/96JC00051

Du Yan, Qu Tangdong. 2010. Three inflow pathways of the Indonesian throughflow as seen from the simple ocean data assimilation. Dynamics of Atmospheres and Oceans, 50(2): 233–256, doi: 10.1016/j.dynatmoce.2010.04.001

England M H, Huang F. 2005. On the interannual variability of the indonesian throughflow and its linkage with ENSO. Journal of Climate, 18(9): 1435–1444, doi: 10.1175/JCLI3322.1

Fang Guohong, Susanto R D, Wirasantosa S, et al. 2010. Volume, heat, and freshwater transports from the South China Sea to Indonesian seas in the boreal winter of 2007–2008. Journal of Geophysical Research: Oceans, 115(C12): C12020, doi: 10.1029/2010JC006225

Godfrey J S. 1989. A Sverdrup model of the depth-integrated flow for the world ocean allowing for island circulations. Geophysical & Astrophysical Fluid Dynamics, 45(1–2): 89–112

Godfrey J S. 1996. The effect of the Indonesian throughflow on ocean circulation and heat exchange with the atmosphere: A review. Journal of Geophysical Research: Oceans, 101(C5): 12217–12237, doi: 10.1029/95JC03860

Gordon A L. 2005. Oceanography of the Indonesian Seas. Oceanography, 18(4): 13, doi: 10.5670/oceanog

Gordon A L, Fine R A. 1996. Pathways of water between the Pacific and Indian oceans in the Indonesian seas. Nature, 379(6561): 146–149, doi: 10.1038/379146a0

Gordon A L, Huber B A, Metzger E J, et al. 2012. South China Sea throughflow impact on the Indonesian throughflow. Geophysical Research Letters, 39(11): L11602

Gordon A L, Sprintall J, Van Aken H M, et al. 2010. The Indonesian throughflow during 2004–2006 as observed by the INSTANT program. Dynamics of Atmospheres and Oceans, 50(2): 115–128, doi: 10.1016/j.dynatmoce.2009.12.002

Hanley D E, Bourassa M A, O'Brien J J, et al. 2003. A quantitative evaluation of ENSO indices. Journal of Climate, 16(8): 1249–1258, doi: 10.1175/1520-0442(2003)16<1249:AQEOEI>2.0.CO;2

Liu Qinyan, Huang Ruixin, Wang Dongxiao, et al. 2006. Interplay between the indonesian throughflow and the South China Sea throughflow. Chinese Science Bulletin, 51(S2): 50–58, doi: 10.1007/s11434-006-9050-x

Liu Qinyan, Feng Ming, Wang Dongxiao, et al. 2015. Interannual variability of the Indonesian Throughflow transport: A revisit based on 30 year expendable bathythermograph data. Journal of Geophysical Research: Oceans, 120(12): 8270–8282, doi: 10.1002/2015JC011351

Luick J L, Cresswell G R. 2001. Current measurements in the Maluku Sea. Journal of Geophysical Research: Oceans, 106(C7): 13953–13958, doi: 10.1029/2000JC000694

Meyers G. 1996. Variation of Indonesian throughflow and the El Niño-Southern oscillation. Journal of Geophysical Research: Oceans, 101(C5): 12255–12263, doi: 10.1029/95JC03729

Miyama T, Awaji T, Akitomo K, et al. 1995. Study of seasonal transport variations in the Indonesian seas. Journal of Geophysical Research: Oceans, 100(C10): 20517–20541, doi: 10.1029/95JC01667

Murray S P, Arief D. 1988. Throughflow into the Indian Ocean through the Lombok Strait, January 1985–January 1986. Nature, 333(6172): 444–447, doi: 10.1038/333444a0

Pujiana K, Gordon A L, Sprintall J, et al. 2009. Intraseasonal variability in Makassar Strait thermocline. Journal of Marine Research, 67(6): 757–777

Qu Tangdong, Du Yan, Meyers G, et al. 2005. Connecting the tropical pacific with Indian Ocean through South China Sea. Geophysical Research Letters, 32(24): L24609, doi: 10.1029/2005GL024698

Qu Tangdong, Du Yan, Sasaki H. 2006. South China Sea throughflow: A heat and freshwater conveyor. Geophysical Research Letters, 33(23): L23617, doi: 10.1029/2006GL028350

Qu Tangdong, Mitsudera H, Yamagata T. 1999. A climatology of the circulation and water mass distribution near the Philippine coast. Journal of Physical Oceanography, 29(7): 1488–1505, doi: 10.1175/1520-0485(1999)029<1488:ACOTCA>2.0.CO;2

Qu Tangdong, Mitsudera H, Yamagata T. 2000. Intrusion of the North Pacific waters into the South China Sea. Journal of Geophysical Research: Oceans, 105(C3): 6415–6424, doi: 10.1029/1999JC900323

Sasaki H, Nonaka M, Masumoto Y, et al. 2008. An eddy-resolving hindcast simulation of the quasiglobal ocean from 1950 to 2003 on the Earth Simulator. In: Hamilton K, Ohfuchi W, eds. High resolution Numerical Modelling of the Atmosphere and Ocean. New York: Springer, 157–185

Sprintall J. 2009. Indonesian Throughflow. In: Thorpe S A, ed. Ocean Currents, a Derivative of Encyclopedia of Ocean Sciences. 2nd ed. London: Elsevier, 237–243

Sprintall J, Gordon A L, Koch-Larrouy A, et al. 2014. The Indonesian seas and their role in the coupled ocean-climate system. Nature Geoscience, 7(7): 487–492, doi: 10.1038/ngeo2188

Susanto R D, Ffield A, Gordon A L, et al. 2012. Variability of Indonesian throughflow within Makassar Strait, 2004–2009. Journal of Geophysical Research: Oceans, 117(C9): C09013

Susanto R D, Gordon A L. 2005. Velocity and transport of the Makassar Strait throughflow. Journal of Geophysical Research: Oceans, 110(C1): C01005

Susanto R D, Wei Zexun, Adi R T, et al. 2013. Observations of the Karimata Strait througflow from December 2007 to November 2008. Acta Oceanologica Sinica, 32(5): 1–6, doi: 10.1007/s13131-013-0307-3

Talley L D, Sprintall J. 2005. Deep expression of the Indonesian Throughflow: Indonesian intermediate water in the South equatorial current. Journal of Geophysical Research: Oceans, 110(C10): C10009, doi: 10.1029/2004JC002826

Tian Jiwei, Yang Qingxuan, Liang Xinfeng, et al. 2006. Observation of Luzon Strait transport. Geophysical Research Letter, 33(19): L19607, doi: 10.1029/2006GL026272

Tozuka T, Qu Tangdong, Masumoto Y, et al. 2009. Impacts of the South China Sea Throughflow on seasonal and interannual variations of the Indonesian Throughflow. Dynamics of Atmospheres and Oceans, 47(1–3): 73–85, doi: 10.1016/j.dynatmoce.2008.09.001

Van Aken H M, Brodjonegoro I S, Jaya I. 2009. The deep-water motion through the Lifamatola Passage and its contribution to the Indonesian throughflow. Deep Sea Research Part I: Oceanographic Research Papers, 56(8): 1203–1216, doi: 10.1016/j.dsr.2009.02.001

Wajsowicz R C. 1993. A simple model of the Indonesian throughflow and its composition. Journal of Physical Oceanography, 23(24): 2683–2703

Wajsowicz R C. 1996. Flow of a western boundary current through multiple straits: An electrical circuit analogy for the Indonesian Throughflow and archipelago. Journal of Geophysical Research: Oceans, 101(C5): 12295–12300, doi: 10.1029/95JC02615

Wang Lu, Xie Lingling, Zhou Lei, et al. 2018. Climatological analysis of water mass sources of Indonesia Throughflow in the Molukka Sea and Halmahera Sea. Haiyang Xuebao (in Chinese), 40(3): 1–15

Wei Zexun, Fang Guohong, Xu Tengfei, et al. 2016a. Seasonal variability of the isopycnal surface circulation in the South China Sea derived from a variable-grid global ocean circulation model. Acta Oceanologica Sinica, 35(1): 11–20, doi: 10.1007/s13131-016-0791-3

Wei Jun, Li M T, Malanotte-Rizzoli P, et al. 2016b. Opposite variability of indonesian Throughflow and South China Sea Throughflow in the Sulawesi Sea. Journal of Physical Oceanography, 46(10): 3165–3180, doi: 10.1175/JPO-D-16-0132.1

Wyrtki K. 1961. Physical Oceanography of the Southeast Asian Waters. In: Naga Report 2. Scripps Institution of Oceanography. La Jolla, California: University of California Press, 2

Xie Lingling, Tian Jiwei, Hu Dunxin, et al. 2009. A quasi-synoptic interpretation of water mass distribution and circulation in the western North Pacific II: Circulation. Chinese Journal of Oceanology and Limnology, 27(4): 630–639

Yuan Dongliang, Zhou Hui, Wang Zheng, et al. 2017. The multi-scale variability of the oceancirculation at the Pacific entrance of the Indonesian Throughflow and its scientific importance. Oceanologia et Limnologia Sinica (in Chinese), (6): 1156–1168

Zhang Yanhui, Yu Xiaolin, Wang Fan. 2008. Origins and pathways of the subsurface and intermediate water masses of the Indonesian Throughflow derived from historical and Argo data. Acta Oceanologica Sinica, 27(4): 17–25

Zhao Yunxia, Wei Zexun, Wang Yonggang, et al. 2015. Correlation analysis of the North Equatorial Current bifurcation and the Indonesian Throughflow. Acta Oceanologica Sinica, 34(9): 1–11, doi: 10.1007/s13131-015-0736-2